Intravoxel incoherent motion and diffusion kurtosis imaging at 3T MRI: Application to ischemic stroke

Aude Pavilla, Giulio Gambarota, Aissatou Signate, Alessandro Arrigo, Hervé Saint-Jalmes, Mehdi Mejdoubi

Intravoxel incoherent motion and diffusion kurtosis imaging at 3T MRI: application to ischemic stroke.

Aude Pavilla[1,2], Giulio Gambarota[1], Aissatou Signaté[2], Alessandro Arrigo[2], Hervé Saint-Jalmes[1], Mehdi Mejdoubi[2]

[1] Univ-Rennes, INSERM, LTSI - UMR 1099, F-35000 Rennes, France.

[2] Département de Neuroradiologie, CHU Martinique, F-97261 Fort de France, France.

Corresponding author: Aude Pavilla, PhD

Département de Neuroradiologie, Hôpital Pierre-Zobda-Quitman, CHU de Martinique CS 90632 – 97261 Fort de France Cedex, France.

Tel: +596 596 55 21 81; Fax: +596 596 75 16 68

email: aude.pavilla@gmail.com

Number of figures and tables: 5 figures and 3 tables

Number of references: 44

Word count: 6694

Keywords: diffusion, perfusion, stroke, intravoxel incoherent motion, kurtosis, brain.

Disclosure of potential conflicts of interest

The authors each declare that they have no conflict of interest.

Abstract

Background and Purpose

The DKI-IVIM model that incorporates DKI (diffusional kurtosis imaging) into the IVIM (Intravoxel Incoherent Motion) concept was investigated to assess its utility for both enhanced diffusion characterization and perfusion measurements in ischemic stroke at 3T.

Methods

Fifteen stroke patients (71±11 years old) were enrolled and DKI-IVIM analysis was performed using 9 b-values from 0 to 1500 s/mm^2 chosen with the Cramer-Rao-Lower-Bound optimization approach. Pseudo-diffusion coefficient D*, perfusion fraction f, blood flow-related parameter fD*, the diffusion coefficient D and an additional parameter, the kurtosis, K were determined in the ischemic lesion and controlateral normal tissue based on a region of interest approach. The apparent diffusion coefficient (ADC) and arterial spin labelling (ASL) cerebral blood flow (CBF) parameters were also assessed and parametric maps were obtained for all parameters.

Results

Significant differences were observed for all diffusion parameters with a significant decrease for D ($p<0.0001$), ADC ($p<0.0001$), and a significant increase for K ($p<0.0001$) in the ischemic lesions of all patients. f decreased significantly in these regions ($p=0.0002$). The fD* increase was not significant ($p=0.56$). The same significant differences were found with a motion correction except for fD* ($p=0.47$). CBF significantly decreased in the lesions. ADC was significantly positively correlated with D ($p< 0.0001$) and negatively with K ($p= 0.0002$); K was also negatively significantly correlated with D ($p = 0.01$).

Conclusions

DKI-IVIM model enables for simultaneous cerebral perfusion and enhanced diffusion characterization in an acceptable clinically acquisition time for the ischemic stroke diagnosis with the additional kurtosis factor estimation, that may better reflect the microstructure heterogeneity.

Introduction

Ischemic brain stroke is mostly related to a large artery occlusion that causes a perfusion impairment and subsequently a tissue infarction through the ischemia cascade mechanisms [1]. IntraVoxel incoherent motion (IVIM) is a magnetic resonance imaging (MRI) concept that allows the separation of perfusion and diffusion effects from diffusion-weighted images [2,3]. Perfusion refers to the oxygen and metabolites delivery through the blood circulation in the capillary bed [4]. Because the capillary network is randomly organized, the collective movement of water molecules in the blood mimics a pseudo diffusion process characterized by a pseudo-diffusion coefficient value approximatively ten times higher than the diffusion coefficient [2,5,6] value. As a result, by using low (typically b<200 s/mm^2) and moderate (typically b up to 1000 s/mm^2) b-values, the two independent perfusion-related and diffusion phenomena can be separated by the classical IVIM model through a theoretical biexponential signal decay fit [7]. Therefore, IVIM offers the opportunity to provide with a minimum additional scan time, perfusion information "for free" [2] in addition to diffusion measurement. Moreover, perfusion is assessed without contrast agent injection required for other perfusion weighted imaging (PWI) modalities[8] namely the dynamic susceptibility contrast (DSC) or the dynamic contrast enhancement (DCE). Because diffusion and perfusion are both altered in the acute phase of ischemic stroke, IVIM represents an appealing noninvasive approach for cerebral ischemic stroke application. In addition, the recent introduction of endovascular mechanical thrombectomy (MT) has marked a paradigm shift in the management of acute ischemic stroke (AIS) [9]. A recent study concluded on the IVIM potential compared to DWI plus ASL to establish a diffusion/perfusion mismatch that may be useful for a rapid triage of the potential MT candidates based on the delineation of their ischemic penumbra and may improve the indication of MT [10]. However, it has been well established that the diffusion process in the biological tissues is not purely gaussian [2,5,11] as considered in most IVIM studies. Among the several models proposed to address this non-gaussian behavior, the Diffusional Kurtosis Imaging (DKI) method includes the estimation of the dimensionless kurtosis coefficient (K) that quantifies the degree of deviation from a gaussian and

reflects somehow the heterogeneity of the tissues diffusion environment [12–14]. This advanced DWI method was initially met with reluctance for clinical management of stroke in terms of additional: 1) scan time needed 2) information provided worth from a clinical perspective. However, these issues have been overcome recently with optimized scan time and promising usefulness of the kurtosis marker for better microstructural changes evaluation following AIS [15–17]. In the current study, following an initial pilot study with only five patients at the lower magnetic field of 1.5T [18], we used an optimized IVIM protocol at 3 teslas (3T) with b-values selection through the Cramer-Rao Lower Bound theory [19] applied to fifteen stroke patients for simultaneous perfusion and diffusion assessment including the kurtosis measurement. The objective of the study was to examine whether the DKI model incorporated into the IVIM model (DKI-IVIM) was capable of simultaneously estimating enhanced diffusion and perfusion characteristics of tissue in brain acute and subacute ischemic stroke with 3T MRI in comparison with the more conventional protocol which includes two separate diffusion (DWI) and perfusion (ASL) sequences.

Material and methods

Patients

This prospective study was approved by the local Ethics Committee "Comité de Protection des Personnes Sud-Ouest et Outre Mer" (CPP15-032). The study was conducted in accordance with the Helsinki Declaration of 1975 as revised in 1983. A total of fifteen stroke patients (9 males and 6 females; mean age 71±11 years, 49-79 range years) who underwent 3.0 T MRI due to acute and subacute[20] hemispheric stroke symptoms were included in the study. The National Institutes of Health Stroke Scale (NIHSS) admission score mean value was 7.7±5.5. Exclusion criteria were: small lesions less than 2 mm in diameter because they are mostly lacunar infarctions, due to a microangiopathy ; important image distortion or motion artifacts on diffusion-weighted images; hemorrhagic stroke transformation.

MRI

MRI scans were performed on a 3T whole-body scanner (MR750W SIGNA, GE Healthcare, Waukesha, WI, USA) using an 8-channel head and neck coil with parallel imaging (acceleration factor, ASSET=2.5). For each patient, standard DWI, IVIM and arterial spin labeling (ASL) sequences were acquired. Additional echo planar imaging T2* (EPI T2*), Fluid-Attenuated inversion recovery (FLAIR), circle of Willis Time of Flight (TOF) MR angiography were also performed for a complete stroke assessment but not quantitatively analyzed in the present study.

For the conventional DWI sequence, parameters were set as follows: TR=8000 ms, TE=79.3 ms, bandwidth=1305 Hz/px, slice thickness of 4 mm, 2 b-values= 0 and 1000 s/mm^2, flip angle=90°, FOV (field-of-view)=240x240 mm^2 and matrix size 140x140, which yielded an in-plane resolution of 1.7x1.7 mm^2. For the DWI sequence used for DKI-IVIM analysis, data were acquired with a single-shot spin-echo EPI (echo planar imaging) with the diffusion-gradients applied in three orthogonal directions (in separate scans) and then averaged. Acquisition parameters were set as follows:

TR/TE=6500/80 ms, bandwidth= 1953 Hz/px, 22 contiguous 4 mm thick axial slices, FOV=240x240 mm^2 and matrix size 128x128, which yielded an in-plane resolution of 1.9x1.9 mm^2 . The optimal b-values distribution was determined by using a CRLB (Cramer-Rao Lower Bound) approach. A figure of merit that estimates the standard deviation of each diffusion (D and K) and perfusion (f and D*) parameters from the DKI-IVIM model was introduced such as follows : $\Gamma_{DKI-IVIM} = \frac{\sigma_D}{D} + \frac{\sigma_K}{K} + \frac{\sigma_f}{f} + \frac{\sigma_{D^*}}{D^*}$.

$\sigma_D, \sigma_K, \sigma_f$ and σ_{D^*} are the CRLB computed values, while D, K, f and D* represent the target values of these parameters chosen in accordance with the literature [21]. The minimization procedure was performed numerically using Mathematica (Wolfram Research Champaign, IL, USA). The required minimum values of five b-values obtained with this procedure was enlarged to nine to improve the robustness whilst having an acceptable scan duration. The maximum b-value was set to 1500 s/mm^2 to ensure sufficient signal-to-noise ratio for proper images interpretation in a clinical context with the DKI-IVIM model [13,14,22]. The full b-values distribution was: 0, 30, 60, 80, 300, 400, 900, 1000 and 1500 s/mm^2 with two averages for b=1500 s/mm^2 and one for the other b-values for a total scan duration of 3 minutes and 9 seconds. Pseudocontinuous 3D ASL (pCASL) was also performed using an interleaved 3D stack of spiral fast-spin echo sequence with background suppression. Multiarm spiral imaging was used, with 8 arms and 512 points acquired on each arm with background suppression. 3D pCASL other parameters were as follows: TR=4854 ms, TE=10.7 ms, post-labeling delay (PLD)= 1525 ms, labeling duration = 1500 ms, pixel bandwidth=977 Hz/pixel, three averages, slice thickness 4.0 mm; FOV=240x240 mm^2 for a total scan duration of approximatively 4 minutes.

Image processing

The conventional DWI and the pCASL data were respectively post-processed to obtain the apparent diffusion coefficient (ADC) and cerebral blood flow (CBF) maps with GE Readyview ® software on an Advantage Windows 4.6 workstation (GE Medical Systems). The DKI-IVIM data post-processing was performed using an in-house script written in MATLAB (Mathworks, MA, USA). For each patient and for every infarction lesion identified on the conventional DWI image with

b=1000 s/mm^2 (hypersignal), a region of interest (ROI) was drawn and reported on the corresponding ADC maps. For all stroke lesions, a mirror ROI was then placed symmetrically in the contralateral healthy hemisphere in the same anatomical locations. The same procedure (lesions and mirrors ROIs) was applied for the images acquired with the DKI-IVIM imaging protocol and the conventional pCASL sequence with volume overlays performed with "MRIcro" Software [23]. Especially for the diffusion images, all the ROIs were carefully placed to exclude contamination by cerebrospinal fluid (CSF) or large vessels. Depending on the stroke volume, for each patient, between eight and twelve ROIs were placed on two or three consecutive slices surrounding the lesion center. One expert neuroradiologist (MM) blinded to the patient information reviewed the MRI images and the ROIs placements. The delineation of the ROIs in stroke areas was chosen on the most relevant images where a hypersignal could be observed. Padding is not always effective in studies involving stroke patients, because remaining motionless in the scanner for a long period of time can be very difficult for these patients, especially for the DKI-IVIM protocol imaging which requires multiple b-value acquisitions. To take in account possible patient motion during the acquisition, a retrospective rigid body motion correction using the FMRIB's linear registration (FLIRT) tool in FSL (FMRIB Software Library; http://www.fmrib.ox.ac.uk/fsl) with 6 degrees of freedom (DOF) and a mutual information cost function was applied to the images acquired with the DKI-IVIM imaging protocol (b=0 s/mm^2 as reference volume). Prior to volumes coregistration with the b=0 s/mm^2 volumes, the DICOM format images of each patient were first converted to NIFTI format and processed with the brain extraction tool (BET) in FSL.

For both DWI motion-corrected and non-motion-corrected images, for a given ROI, signal averaging was performed at each b value across pixels before performing the fit with the DKI-IVIM model.

For this ROI approach, a constrained fitting method as reported elsewhere [24,25]. Based on the nine acquired b-values, a two-steps segmented non-gaussian fit was used to estimate the DKI-IVIM indexes: 1) diffusion parameters: the kurtosis K, a measure of the excess kurtosis of diffusion and the mean diffusion coefficient D that takes in account this non-gaussian behavior; and 2) perfusion parameters: the fraction of perfusion f and D*, the pseudo-diffusion coefficient of the water in blood at the capillary level in tissues.

D and K were first obtained by fitting the signals obtained with b=300-1500 s/mm^2 with a mono-exponential function given that the IVIM effect is negligible in this regime:

$$\frac{S(b > 300\ s/mm^2)}{S_{int}} = \exp(-bD + \frac{b^2D^2K}{6})$$

S_{int}, is the intercept of the diffusion-related signal (b > 300 s/mm^2) with the y-axis (in other terms, the value of the signal at b = 0 s/ mm^2 if no pseudo-diffusion component was present).

In a second step, the perfusion (f and D*) parameters were obtained by fitting all the data points using the D and K values from the first step using the following equation based on the DKI-IVIM model : $\frac{S(b)}{S_0} = f\exp(-\mathrm{b}D^*) + (1 - \mathrm{f})\exp(-bD + \frac{b^2D^2K}{6})$ where S_0 is the signal intensity at b=0 s/mm^2.

To generate diffusion (D and K) and perfusion (f and the scalar multiplication fD* product) parametric maps, the previous equation was also fitted by a segmented method based on a pixel-wise approach using the DKI-IVIM model with a Trust-Region algorithm [26]. To enhance the precision of D* and f for the perfusion maps, the perfusion fraction f was assessed using by the y-intercept of the signal line above b=300s/mm^2 and the pseudodiffusion coefficient D* was obtained from the monoexponential fit using the pre-calculated D, K and f values as reported elsewhere [24].

In both ROI and pixel-by-pixel approaches, for perfusion, values with f greater than 0.3 and values with D* greater than 0.1 mm^2/s were arbitrarily set to zero. These values were considered as not physiological and can be interpreted as contamination from partial volume with the cerebrospinal fluid (CSF) or noise in a vanishing perfusion component [21]. All the ischemic lesions and hypoperfused territories delimitations were manually drawn after thresholding with visual inspection performed by the expert neuroradiologist (MM).

Statistical analysis

ADC, CBF and DKI-IVIM parameters were averaged over all patients in the affected and contralateral areas and reported as mean ± standard deviation. The paired Student t-test was used to compare the mean values of each parameter in the lesions and contralateral healthy regions. The Pearson correlation analysis was performed for all the subjects to explore potential relationships between the conventional ADC, CBF and DKI-IVIM parameters in both affected and contralateral

regions. Statistical analyses were performed using GraphPad Prism version 9.0 (GraphPad software, Inc., La Jolla, CA, USA). A threshold of $p<0.05$ was used to define statistical significance.

Results

Patients demographics are reported in **Table 1**. For each patient, all data analysis were well performed. An example of the signal intensity plotted as a function of b-values for a region of interest (ROI) located in the ischemic area and a ROI in the healthy contralateral area is shown on **Figure 1**. DWI-IVIM axial images for two patients with a confirmed stroke diagnosis and the corresponding DKI-IVIM parametric maps are presented on **Figure 2 and 3**.

The mean values for all diffusion and perfusion parameters in the lesions and normal contralateral areas for all patients are reported in **Table 2**. The paired Student t-test used on the data prior to motion correction revealed significant differences for all the diffusion parameters with a significant decrease for D ($p<0.0001$) and a significant increase for K ($p<0.0001$) in the ischemic lesions. f decreased significantly in the ischemic regions ($p=0.0002$). An increase but not significant in fD* values was found ($p=0.56$) in the infarct area probably due to a high variance on D* measurement. The paired Student t-test revealed also the same significant differences with the applied motion correction for all DKI-IVIM parameters except for fD* with a non-significant decrease ($p =0.47$) observed in the ischemic areas.

In order to minimize the post-processing procedure for a clinical perspective, the non-motion corrected data were used for further investigations as no significant differences were observed between all the DKI-IVIM diffusion and perfusion parameters obtained prior and after motion correction. All the mean DKI-IVIM parameters values before and after the motion correction application averaged over all the patients in addition to the corresponding mean ADC and CBF patients values are reported on **Figure 4**. Regarding the conventional diffusion and perfusion parameters, a significant decrease in the ADC values ($x10^{-3}$ mm^2/s) ($ADC=0.49\pm0.01$ vs. $ADC=0.78\pm0.01$, $p<0.0001$) and the CBF values (in mL/min/100g) estimated by ASL ($CBF=28.3\pm12.6$ vs. $CBF=41.0\pm10.1$, $p<0.0001$) was observed in

the lesions. The coefficients of correlation between the mean values of ADC and DKI-IVIM parameters values averaged over all the patients are shown in **Table 3**. In both lesions and contralateral areas, the ADC was significantly positively correlated with D and significantly negatively correlated with K.

No significant correlations were found between ADC, f and fD* parameters (p=0.16 and p=0.26 respectively) or between the CBF-ASL and the blood-flow related fD* (p=0.77) parameter. The scatter plots for relationships between the ADC and the diffusion DKI-IVIM parameters D and K are shown in **Figure 5**. Additionally, a significant negative correlation was found between these two diffusion DKI-IVIM parameters (r=-0.330 p=0.01).

Discussion

We showed that DKI-IVIM was able to measure simultaneously advanced diffusion and perfusion tissues properties in acute and subacute cerebral ischemic stroke patients. This is performed with a 3 minutes and 9 seconds sequence compared to the average 3 to 5 minutes needed in the standard stroke protocol for the distinct conventional DWI (1min) plus PWI (1min40s) or DWI (1min) plus ASL (4min) sequences [27].

Simultaneous diffusion and perfusion estimation with IVIM

A preliminary study reported the feasibility of measuring simultaneously cerebral perfusion and diffusion with DKI-IVIM in the acute phase of ischemic stroke at 1.5T [18]. Although the measurements obtained for the diffusion were found consistent with a restricted diffusion in stroke lesions, the perfusion estimations were found with limited robustness highlighting the need for higher SNR provided by 3T MRI.

In this study conducted at 3T, we showed that the curves of the diffusion-weighted signal intensity versus b-value were still well fitted beyond 1000 s/mm^2 with the non-gaussian DKI-IVIM bi-exponential model in both ischemic and normal contralateral tissues with a maximum b-value set at 1500 s/mm^2.

A previous study also demonstrated with the Akaike criteria that the same model with the maximum b-value set at 1500 s/mm^2 was able to measure accurately a hypoperfusion induced by a hyperventilation challenge, in a healthy cohort using a 4 minutes DWI-based protocol imaging at 1.5T [22]. Initially proposed by Le Bihan et al, IVIM imaging is a variant of the conventional DWI where the signal is acquired at multiple b-values and fitted with a two-compartment biexponential model to separate the microcirculatory blood flow and the water diffusion in the interstitial space [2,7]. MR

hardware improvements and pulse sequences advances have played an important role for the IVIM revival this last decade. This method has been successfully applied in several body organs and in the human brain in recent studies [14,28–31].

Kurtosis non-gaussian diffusion analysis with DKI-IVIM model. Enhanced diffusion characterization

Although encouraging, most of these studies did not account for the non-Gaussian diffusion behavior that is accounted for in the diffusional kurtosis imaging. Moreover, in some of them [14,31], no comparison was performed with another perfusion method, either DSC or DCE (using both gadolinium injection) or ASL. Thereby, feasibility studies using hybrid DKI and IVIM and comparison with standard diffusion and another perfusion MR modality remain relatively scarce in human brain studies [22,25,32,33]. Also, the demanding signal to noise ratio (SNR) required for both IVIM imaging and the higher maximum b-value needed to perform DKI analysis may explain the challenging application of this model especially for acute stroke diagnosis where the imaging protocol should be as short as possible [15,34]. Nevertheless, hybrid IVIM and DKI imaging has shown to be a promising noninvasive method for quantifying human brain diffusion and microvascular perfusion of the human brain, but to date, only feasibility studies on brain tumors have been reported [25,35]. To the best of our knowledge DKI-IVIM application study on human brain ischemic stroke with ASL perfusion measurements comparison at 3T has not been performed so far.

Sequence design and motion correction influence

The DWI-based sequence acquisition for DKI-IVIM analysis requires many scans in multiple diffusion directions and for different b-values. Because stroke patients can frequently experiment head motion during the MRI scans and small changes between b-values acquisitions can lead to image artifacts, in the current study, motion was corrected by using a two-dimensional (in-plane) image registration algorithm with the b=0 s/mm^2 images as a reference. Non-corrected and motion corrected data were then compared. In both cases, the diffusion parameters (D and K) and the perfusion-related f parameter showed significant differences between the ischemic and healthy contralateral regions, but

the decreasing trend of fD* was only observed in the affected region with the motion correction application. Our results indicated that motion corrected or not corrected data seem to be comparable for detecting significant changes in this small cohort. However, it is difficult to generalize this specific observation here, further investigations on larger cohorts would be needed to justify using or not using motion correction for a clinical use. However, as time is a crucial parameter in the acute phase of ischemic stroke, an optimized DKI-IVIM pipeline study that minimize both b-values acquisitions and post-processing procedures should be preferred.

Ischemic stroke application

Our results were consistent with recent stroke studies at 3T with conventional IVIM method in the brain, which showed a decrease of the IVIM diffusion (D) and perfusion (f) parameters while DKI studies found an increase of the kurtosis factor in the ischemic lesions [20,21,29]. Restricted diffusion in the affected area can explain lower D values as reported elsewhere [16,17]. The perfusion fraction f measured by IVIM imaging reflects within each voxel the volume fraction of capillary blood flow. Vascular occlusion that occurs in stroke impairs the capillary transport of oxygen and nutrients and may alter the microvasculature causing the f decrease observed in the infarct core. Moreover, it has been demonstrated that non gaussian diffusion affects the signal at high b-values and impact on low b-values as IVIM effects are small [2]. Of the two IVIM-derived perfusion indexes, the blood volume fraction f was found more robust than the pseudo-diffusion coefficient D* and the subsequently blood flow related fD* product as widely reported. Federau et al. [21] considered only the results of the perfusion fraction f and not those of the pseudo-diffusion coefficient D*, as it is well supported that the interpretation of this parameter is very challenging because it represents a vanishing compartment diffusion coefficient [2,36]. Furthermore, if the diffusion is not well fitted, possible misestimation of perfusion IVIM parameters can occur because the two phenomena are not fully independent. For instance, f has been shown overestimated with the biexponential IVM model if b>1000s/mm^2 [2]. Our f values estimated through the hybrid DKI-IVIM were effectively found lower in both ischemic and healthy brain tissues in comparison to studies using the biexponential IVIM model [20,21].

Supplementary information provided by kurtosis estimations

Evidence of a deviation from a gaussian diffusion can be assessed by the kurtosis factor in vivo. In the DKI model, the kurtosis measures, within a given imaging voxel, a basic physical property of the microscopic environment distribution of the water molecules displacement (12,15).

Healthy brain tissues have a kurtosis value of around 1 [37]. K value increases due to the microstructural tissues complexity (components, diffusion barriers) [13]. In other terms, the mean kurtosis can reflect the complexity of tissue structure which represents an opportunity for ischemic stroke lesions heterogeneity characterization [15]. Most of these studies concluded that K metrics can provide more abundant information than conventional MRI with K being more sensitive to sub-acute stroke changes than ADC [38]. Investigations on white matter suggested that DKI could provide potential information on the orientation of the structural changes with more pronounced alterations in the axial direction rather than the radial direction [16]. Cheung et al. [39] used a model of middle cerebral artery occlusion in rats and found the interest of the kurtosis for improved sensitivity and specificity in neural tissues diffusion characterization for white matter and especially grey matter in which almost isotropic diffusion generally make advanced methods such as DTI useless. Arguments for the K increase are related to the sharp drop in the axial diffusivity due to axonal varicosities and endoplasmic reticulum abnormalities [15,40]. Our results tend to confirm these hypotheses with the significant negative correlation found between mean K and D or ADC. Pixel-by-pixel maps reconstruction represents probably a better way to visualize the lesions heterogeneity. The maps obtained suggested, as other studies [25,37,39] that a D and K mismatch investigation would be valuable. Stroke preclinical studies found that tissues with a ADC and K mismatch in the lesions were less likely to recover at reperfusion [37]. If the same results were to be found in acute ischemic stroke patients, DKI could be a promising tool to guide MT triage with a more pertinent penumbra evaluation of tissues to be salvaged. Moreover, DKI could be considered as a complement of existing stroke methods to elucidate possible biophysical mechanisms of functional tissue restoration after stroke. These conclusions were also supported by other preclinical studies in which a lower pH were found in kurtosis lesions (K>1) [41,42]. These findings reinforce the idea that DKI has the potential to reveal the heterogeneity and the cellular metabolic impairment complementary to the common DWI assessments [15,16].

Comparison with ASL

An advantage of IVIM is that the quantification of the perfusion is locally assessed and not directly dependent on large arteries unlike the arterial spin labeling (ASL) technique, which is the only perfusion MR modality that does not require the injection of a contrast agent [43].

Our data showed no significant correlation between fD* and the CBF estimated with ASL. The large fD* variance is likely to due to low D* precision. Nevertheless, it is very difficult to be conclusive on fD* and ASL correlation because few studies comparing these two parameters are available for stroke. Wu and al. [34] found no correlation between these two parameters in eighteen healthy patients. Yao and al. [44] found a weak correlation in thirty-eight stroke patients. More recently Zhu and al. found a good agreement between IVIM fD* and ASL parameters changes in stroke patients with large vessel occlusion [10].

Limits

Our study suffers from some limitations. First, the cohort size studied was rather small. Second, inter- and intra-observer reproducibility were not studied. Third, it should be remembered that direct comparison of IVIM with ASL might be cautious because IVIM reflects local flow blood within the imaging voxel, whereas ASL quantifies the transit of blood that has been labeled downstream of the imaging voxel [2]. In addition, with the ASL technique, the presence of an occlusion at the large vessels level can also represent an issue for proper quantification due to uncertain delayed transit time estimation before the perfusion assessment in an upstream imaging voxel [8,43]. Infarct core mean diffusion, kurtosis and perfusion fraction f volumes assessments have to be further estimated for possible DKI-IVIM diffusion-perfusion mismatch investigations.

Conclusions

Diffusional Kurtosis Imaging incorporation (DKI) to the Intravoxel incoherent motion (IVIM) model has the potential to provide non-invasively and simultaneously enhanced diffusion and perfusion information in the context of acute and subacute ischemic stroke. Hybrid DKI-IVIM imaging protocol requires only a minimal additional scan time on a specifically designed DWI sequence and does not require any contrast agent injection. The kurtosis factor provided by DKI-IVIM is promising for more detailed assessment of pathologic tissue changes.

Declaration of interest:

None.

References

1. Powers WJ. Acute Ischemic Stroke. Solomon CG, ed. *N Engl J Med*. 2020;383(3):252-260. doi:10.1056/NEJMcp1917030

2. Le Bihan D. What can we see with IVIM MRI? *NeuroImage*. 2019;187:56-67. doi:10.1016/j.neuroimage.2017.12.062

3. Le Bihan D. Intravoxel Incoherent Motion Perfusion MR Imaging: A Wake-Up Call [1]. *Radiology*. 2008;249(3):748-752. doi:10.1148/radiol.2493081301

4. Markus HS. Cerebral perfusion and stroke. *J Neurol Neurosurg Psychiatry*. 2004;75(3):353-361. doi:10.1136/jnnp.2003.025825

5. Le Bihan D. Apparent Diffusion Coefficient and Beyond: What Diffusion MR Imaging Can Tell Us about Tissue Structure. *Radiology*. 2013;268(2):318-322. doi:10.1148/radiol.13130420

6. Suzuki K, Igarashi H, Watanabe M, Nakamura Y, Nakada T. Separation of Perfusion Signals from Diffusion-Weighted Image Series Enabled by Independent Component Analysis. *J Neuroimaging*. 2011;21(4):384-394. doi:10.1111/j.1552-6569.2010.00514.x

7. Le Bihan D, Breton E, Lallemand D, Aubin ML, Vignaud J, Laval-Jeantet M. Separation of diffusion and perfusion in intravoxel incoherent motion MR imaging. *Radiology*. 1988;168(2):497-505. doi:10.1148/radiology.168.2.3393671

8. Barbier EL, Lamalle L, Décorps M. Methodology of brain perfusion imaging: Methodology of Brain Perfusion Imaging. *J Magn Reson Imaging*. 2001;13(4):496-520. doi:10.1002/jmri.1073

9. Campbell BCV, Mitchell PJ, Kleinig TJ, et al. Endovascular Therapy for Ischemic Stroke with Perfusion-Imaging Selection. *N Engl J Med*. 2015;372(11):1009-1018. doi:10.1056/NEJMoa1414792

10. Zhu G, Federau C, Wintermark M, et al. Comparison of MRI IVIM and MR perfusion imaging in acute ischemic stroke due to large vessel occlusion. *Int J Stroke*. 2020;15(3):332-342. doi:10.1177/1747493019873515

11. Grinberg F, Farrher E, Ciobanu L, Geffroy F, Le Bihan D, Shah NJ. Non-Gaussian Diffusion Imaging for Enhanced Contrast of Brain Tissue Affected by Ischemic Stroke. Harel N, ed. *PLoS ONE*. 2014;9(2):e89225. doi:10.1371/journal.pone.0089225

12. Jensen JH, Helpern JA, Ramani A, Lu H, Kaczynski K. Diffusional kurtosis imaging: The quantification of non-gaussian water diffusion by means of magnetic resonance imaging. *Magn Reson Med*. 2005;53(6):1432-1440. doi:10.1002/mrm.20508

13. Jensen JH, Helpern JA. MRI quantification of non-Gaussian water diffusion by kurtosis

analysis. *NMR Biomed*. 2010;23(7):698-710. doi:10.1002/nbm.1518

14. Bai Y, Lin Y, Tian J, et al. Grading of Gliomas by Using Monoexponential, Biexponential, and Stretched Exponential Diffusion-weighted MR Imaging and Diffusion Kurtosis MR Imaging. *Radiology*. 2016;278(2):496-504. doi:10.1148/radiol.2015142173

15. Rosenkrantz AB, Padhani AR, Chenevert TL, et al. Body diffusion kurtosis imaging: Basic principles, applications, and considerations for clinical practice: Body Diffusion Kurtosis Imaging. *J Magn Reson Imaging*. 2015;42(5):1190-1202. doi:10.1002/jmri.24985

16. Hui ES, Fieremans E, Jensen JH, et al. Stroke Assessment With Diffusional Kurtosis Imaging. *Stroke*. 2012;43(11):2968-2973. doi:10.1161/STROKEAHA.112.657742

17. Weber RA, Hui ES, Jensen JH, et al. Diffusional Kurtosis and Diffusion Tensor Imaging Reveal Different Time-Sensitive Stroke-Induced Microstructural Changes. *Stroke*. 2015;46(2):545-550. doi:10.1161/STROKEAHA.114.006782

18. Pavilla A, Gambarota G, Arrigo A, Saint-Jalmes H, Mejdoubi M. Toward an Intravoxel Incoherent Motion 2-in-1 Magnetic Resonance Imaging Sequence for Ischemic Stroke Diagnosis? An Initial Clinical Experience With 1.5T Magnetic Resonance. *J Comput Assist Tomogr*. 2022;46(1):110-115. doi:10.1097/RCT.0000000000001243

19. Leporq B, Saint-Jalmes H, Rabrait C, et al. Optimization of intra-voxel incoherent motion imaging at 3.0 Tesla for fast liver examination: Optimization of Liver Motion Imaging at 3.0T. *J Magn Reson Imaging*. 2015;41(5):1209-1217. doi:10.1002/jmri.24693

20. Suo S, Cao M, Zhu W, et al. Stroke assessment with intravoxel incoherent motion diffusion-weighted MRI: Ivim Diffusion-Weighted Mri for Human Stroke. *NMR Biomed*. 2016;29(3):320-328. doi:10.1002/nbm.3467

21. Federau C, Sumer S, Becce F, et al. Intravoxel incoherent motion perfusion imaging in acute stroke: initial clinical experience. *Neuroradiology*. 2014;56(8):629-635. doi:10.1007/s00234-014-1370-y

22. Pavilla A, Gambarota G, Arrigo A, Mejdoubi M, Duvauferrier R, Saint-Jalmes H. Diffusional kurtosis imaging (DKI) incorporation into an intravoxel incoherent motion (IVIM) MR model to measure cerebral hypoperfusion induced by hyperventilation challenge in healthy subjects. *Magn Reson Mater Phys Biol Med*. 2017;30(6):545-554. doi:10.1007/s10334-017-0629-9

23. Rorden C, Brett M. Stereotaxic Display of Brain Lesions. *Behav Neurol*. 2000;12(4):191-200. doi:10.1155/2000/421719

24. Suo S, Lin N, Wang H, et al. Intravoxel incoherent motion diffusion-weighted MR imaging of breast cancer at 3.0 tesla: Comparison of different curve-fitting methods: Different IVIM Analyses in Breast Cancer. *J Magn Reson Imaging*. 2015;42(2):362-370. doi:10.1002/jmri.24799

25. Wu WC, Yang SC, Chen YF, Tseng HM, My PC. Simultaneous assessment of cerebral blood volume and diffusion heterogeneity using hybrid IVIM and DK MR imaging: initial experience with brain tumors. *Eur Radiol*. Published online February 23, 2016. doi:10.1007/s00330-016-4272-z

26. Coleman TF, Li Y. An Interior Trust Region Approach for Nonlinear Minimization Subject to Bounds. *SIAM J Optim*. 1996;6(2):418-445. doi:10.1137/0806023

27. González RG. Clinical MRI of acute ischemic stroke. *J Magn Reson Imaging*. 2012;36(2):259-271. doi:10.1002/jmri.23595

28. Cho GY, Moy L, Kim SG, et al. Evaluation of breast cancer using intravoxel incoherent motion (IVIM) histogram analysis: comparison with malignant status, histological subtype, and molecular prognostic factors. *Eur Radiol*. 2016;26(8):2547-2558. doi:10.1007/s00330-015-4087-3

29. Federau C, O'Brien K, Meuli R, Hagmann P, Maeder P. Measuring brain perfusion with intravoxel incoherent motion (IVIM): initial clinical experience. *J Magn Reson Imaging JMRI*. 2014;39(3):624-632. doi:10.1002/jmri.24195

30. Wang P, Thapa D, Wu G, Sun Q, Cai H, Tuo F. A study on diffusion and kurtosis features of cervical cancer based on non-Gaussian diffusion weighted model. *Magn Reson Imaging*. 2018;47:60-66. doi:10.1016/j.mri.2017.10.016

31. Luciani A, Vignaud A, Cavet M, et al. Liver cirrhosis: intravoxel incoherent motion MR imaging--pilot study. *Radiology*. 2008;249(3):891-899. doi:10.1148/radiol.2493080080

32. Liao YP, Urayama S ichi, Isa T, Fukuyama H. Optimal Model Mapping for Intravoxel Incoherent Motion MRI. *Front Hum Neurosci*. 2021;15:617152. doi:10.3389/fnhum.2021.617152

33. De Luca A, Bertoldo A, Froeling M. Effects of perfusion on DTI and DKI estimates in the skeletal muscle: Effects of Perfusion on DTI and DKI in Muscle. *Magn Reson Med*. Published online August 2016. doi:10.1002/mrm.26373

34. Wu WC, Chen YF, Tseng HM, Yang SC, My PC. Caveat of measuring perfusion indexes using intravoxel incoherent motion magnetic resonance imaging in the human brain. *Eur Radiol*. 2015;25(8):2485-2492. doi:10.1007/s00330-015-3655-x

35. Fujima N, Sakashita T, Homma A, Yoshida D, Kudo K, Shirato H. Utility of a Hybrid IVIM-DKI Model to Predict the Development of Distant Metastasis in Head and Neck Squamous Cell Carcinoma Patients. *Magn Reson Med Sci*. 2018;17(1):21-27. doi:10.2463/mrms.mp.2016-0136

36. Federau C. Intravoxel incoherent motion MRI as a means to measure *in vivo* perfusion: A review of the evidence. *NMR Biomed*. 2017;30(11):e3780. doi:10.1002/nbm.3780

37. Jensen JH. Advanced DWI Methods for the Assessment of Ischemic Stroke. *Am J Roentgenol*. 2018;210(4):728-730. doi:10.2214/AJR.17.19223

38. Fung SH, Roccatagliata L, Gonzalez RG, Schaefer PW. MR Diffusion Imaging in Ischemic Stroke. *Neuroimaging Clin N Am*. 2011;21(2):345-377. doi:10.1016/j.nic.2011.03.001

39. Wu EX, Cheung MM. MR diffusion kurtosis imaging for neural tissue characterization. *NMR Biomed*. 2010;23(7):836-848. doi:10.1002/nbm.1506

40. Jensen JH, Falangola MF, Hu C, et al. Preliminary observations of increased diffusional kurtosis in human brain following recent cerebral infarction. *NMR Biomed*. 2011;24(5):452-457. doi:10.1002/nbm.1610

41. Wang E, Wu Y, Cheung JS, et al. pH imaging reveals worsened tissue acidification in diffusion kurtosis lesion than the kurtosis/diffusion lesion mismatch in an animal model of acute stroke. *J Cereb Blood Flow Metab*. 2017;37(10):3325-3333. doi:10.1177/0271678X17721431

42. Lu D, Jiang Y, Ji Y, et al. JOURNAL CLUB: Evaluation of Diffusion Kurtosis Imaging of Stroke Lesion With Hemodynamic and Metabolic MRI in a Rodent Model of Acute Stroke. *Am J Roentgenol*. 2018;210(4):720-727. doi:10.2214/AJR.17.19134

43. Detre JA, Alsop DC. Perfusion magnetic resonance imaging with continuous arterial spin labeling: methods and clinical applications in the central nervous system. *Eur J Radiol*. 1999;30(2):115-124.

44. Yao Y, Zhang S, Tang X, et al. Intravoxel incoherent motion diffusion-weighted imaging in stroke patients: initial clinical experience. *Clin Radiol*. 2016;71(9):938.e11-938.e16. doi:10.1016/j.crad.2016.04.019

Tables

Table 1

Demographics

Patient no.	Gender	Age	NIHSS score	Stroke location	Side	Stroke onset to MRI
1	M	74	8	MCA	Left	<6h
2	F	66	10	MCA	Left	<6h
3	M	76	5	MCA	Left	<6h
4	M	77	4	MCA	Right	<6h
5	M	50	5	AChA	Right	<6h
6	F	75	8	MCA	Right	>6h
7	F	52	3	MCA	Right	<6h
8	F	78	11	MCA	Left	<6h
9	M	78	5	MCA	Left	6 days
10	F	49	7	MCA	Right	>6h
11	F	72	5	MCA	Left	4 days
12	M	79	3	MCA	Left	<6h
13	M	77	18	MCA	Right	<6h
14	M	81	21	MCA/ ACA	Left	>6h
15	M	75	2	MCA	Left	>6H

MCA: Middle cerebral artery

ACA: Anterior cerebral artery

(AChA) : Anterior choroidal artery

Table 2

Comparison of diffusion and perfusion measurements in the ischemic and contralateral healthy tissues prior and after motion correction.

Data are presented as mean ± standard deviation.

	ROI	D ($10^{-3}mm^2/s$)	K	f	fD* ($10^{-3}mm^2/s$)
Prior to motion correction	**Ischemic lesion**	0.58 ± 0.02	1.29 ± 0.52	0.025 ± 0.027	0.60 ± 0.85
	Control	0.93 ± 0.01	0.80 ± 0.30	0.043 ± 0.038	0.52 ± 0.53
	p value	<0.0001†	<0.0001†	0.0002†	0.56
Motion correction	**Ischemic lesion**	0.54 ± 0.01	1.19 ± 0.66	0.027 ± 0.023	0.37 ± 0.42
	Control	0.92 ± 0.01	0.82 ± 0.24	0.039 ± 0.029	0.45 ± 0.49
	p value	<0.0001†	0.0027†	0.026†	0.47

† Significant p-value

Table 3

Pearson correlations between mean values of ADC and DKI-IVIM parameters obtained from all subjects in both ischemic and healthy contralateral tissues.

	D ($10^{-3}mm^2/s$)	K	f	fD* ($10^{-3}mm^2/s$)
r	0.599	0.467	0.182	-0.147

p value	<0.0001*	0.0002*	0.16	0.26

* Significant p-value

Figures legends

Figure 1 *(COLOR)*

Example of region of interest (ROI) delineations on a DWI-IVIM image (b=1000 s/mm^2). (a) ROI delineation of the ischemic lesion and the corresponding healthy tissues. (b) Signal intensity plot as a

function of b-values for the average signal of the pixels in the ROIs placed in the affected and healthy hemispheres.

Figure 2 *(COLOR)*

77-year-old male with stroke of the left middle cerebral artery territory. DKI-IVIM (a) diffusion-weighted image (b=1000 s/mm^2) and derived parameter maps: (b) D, (c) K, (d) f, (e) fD* perfusion related maps. Restricted diffusion on the D map and associated mean kurtosis factor increase on the K map are shown in the same territory. The hypoperfusion area is visible on the (d) f and (e) fD* maps. The lesion is also observed on the conventional (f) diffusion-weighted image (b =1000 s/mm^2), (g) ADC map, (h) T_2 FLAIR image. The time-of-flight MR angiography shows an occlusion of the left middle cerebral artery, the hypoperfusion is also observed on the CBF (j) map.

Figure 3 *(COLOR)*

f

79-year-old male with stroke in the right anterior middle cerebral territory. DKI-IVIM (a) diffusion-weighted image (b=1000 s/mm^2) and derived parameter maps: (b) D, (c) K, (d) f, (e) fD* perfusion related maps. Restricted diffusion on the D map and associated mean kurtosis factor increase on the K map are shown in the same territory. The hypoperfusion area is visible on the (d) f and (e) fD* maps. The lesion is also observed on the conventional (f) diffusion-weighted image (b =1000 s/mm^2), (g) ADC map, (h) T_2 FLAIR image. The time-of-flight MR angiography shows an occlusion of the right middle cerebral artery, the hypoperfusion is also observed on the CBF (j) map.

Figure 4

(a) Comparison of DKI-IVIM parameters between ischemic areas and contralateral healthy tissues before and after motion correction.

(b) Comparison of ADC and CBF parameters between ischemic areas and contralateral healthy tissues.

Figure 5

Scatter plots and Pearson correlation coefficients between ADC and IVIM diffusion parameters D and K: ADC versus D (a), ADC versus K (b) and between K and D (c). Data points are mean values from the whole lesion and contralateral ROIs across all the patients.

Figure 1

Example of region of interest (ROI) delineations on a DWI-IVIM image (b=1000 s/mm^2). (a) ROI delineation of the ischemic lesion and the corresponding healthy tissues. (b) Signal intensity plot as a function of b-values for the average signal of the pixels in the ROIs placed in the affected and healthy hemispheres.

(a)

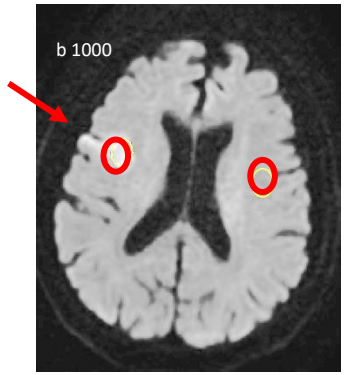

(b)

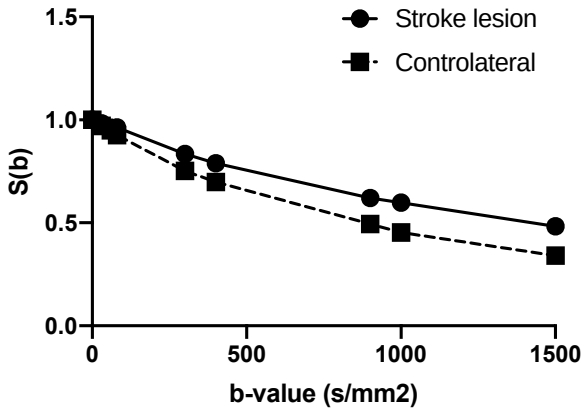

Figure 2

77-year-old male with stroke of the left middle cerebral artery territory. DKI-IVIM (a) diffusion-weighted image (b=1000 s/mm^2) and derived parameter maps: (b) D, (c) K, (d) f, (e) fD* perfusion related maps. Restricted diffusion on the D map and associated mean kurtosis factor increase on the K map are shown in the same territory. The hypoperfusion area is visible on the (d) f and (e) fD* maps. The lesion is also observed on the conventional (f) diffusion-weighted image (b =1000 s/mm^2), (g) ADC map, (h) T_2 FLAIR image. The time-of-flight MR angiography shows an occlusion of the left middle cerebral artery, the hypoperfusion is also observed on the CBF (j) map

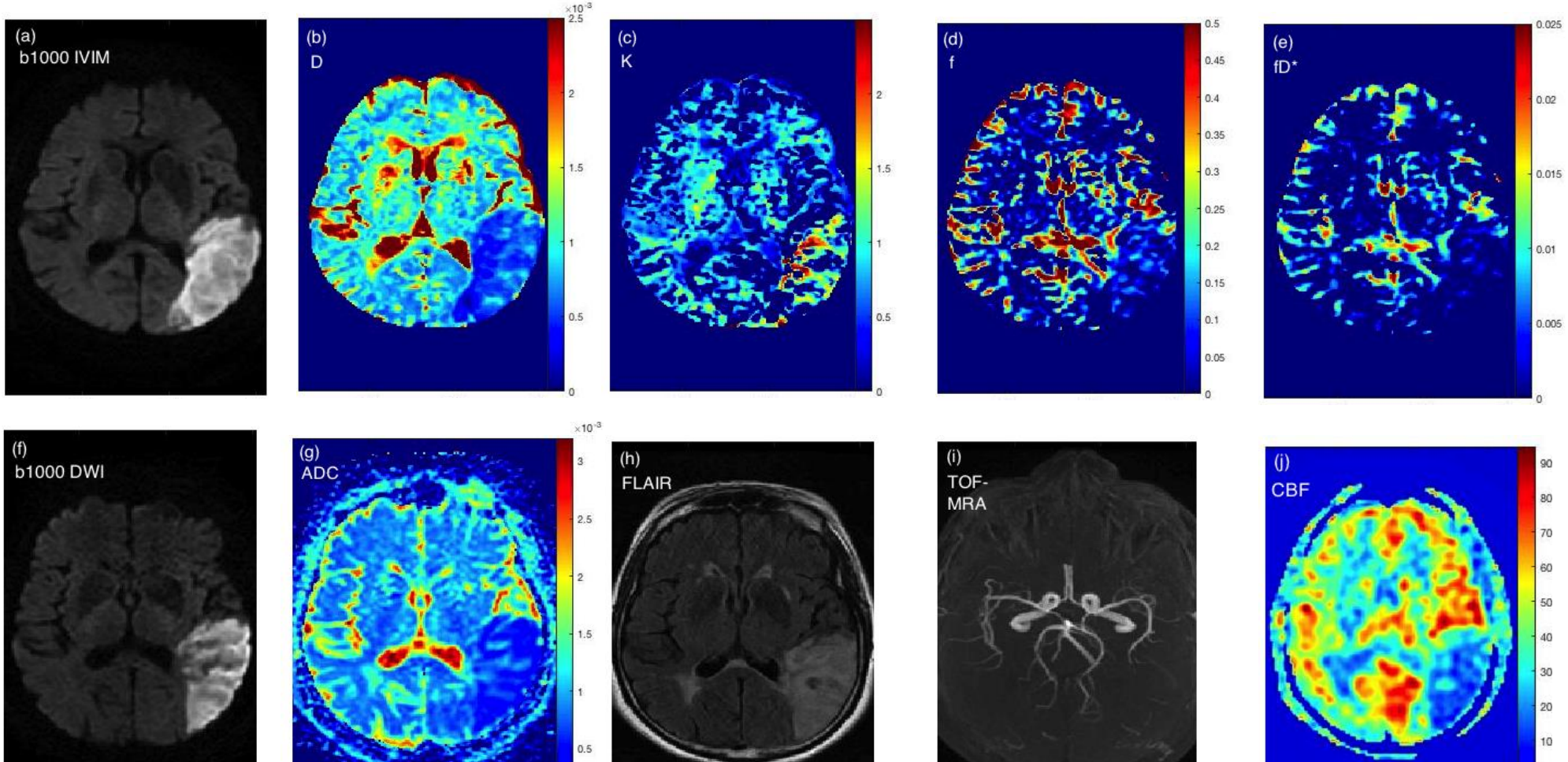

Figure 3

79-year-old male with stroke in the right anterior middle cerebral territory. DKI-IVIM (a) diffusion-weighted image (b=1000 s/mm^2) and derived parameter maps: (b) D, (c) K, (d) f, (e) fD* perfusion related maps. Restricted diffusion on the D map and associated mean kurtosis factor increase on the K map are shown in the same territory. The hypoperfusion area is visible on the (d) f and (e) fD* maps. The lesion is also observed on the conventional (f) diffusion-weighted image (b =1000 s/mm^2), (g) ADC map, (h) T_2 FLAIR image. The time-of-flight MR angiography shows an occlusion of the right middle cerebral

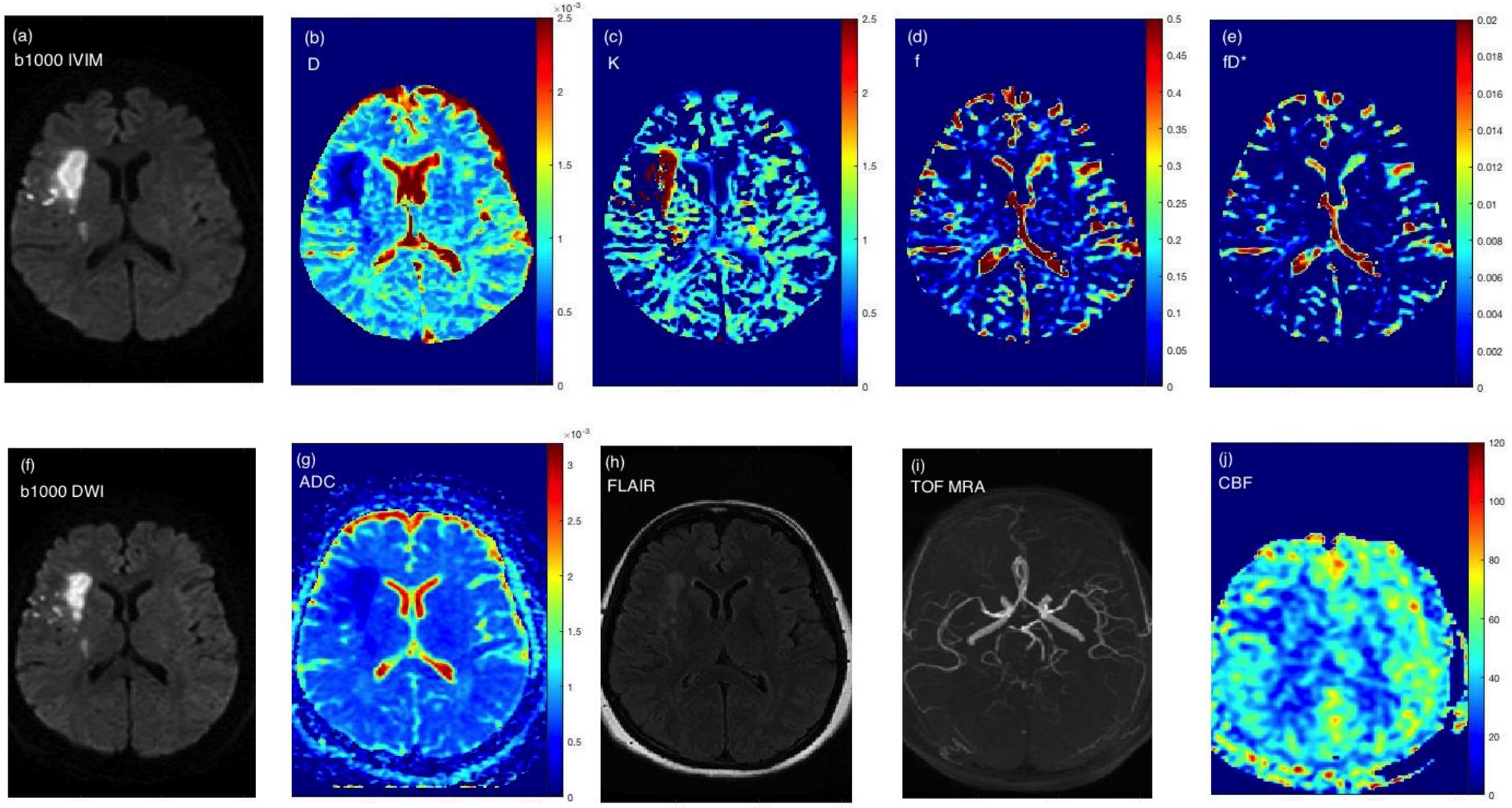

artery, the hypoperfusion is also observed on the CBF (j) map.

Figure 4

(a)

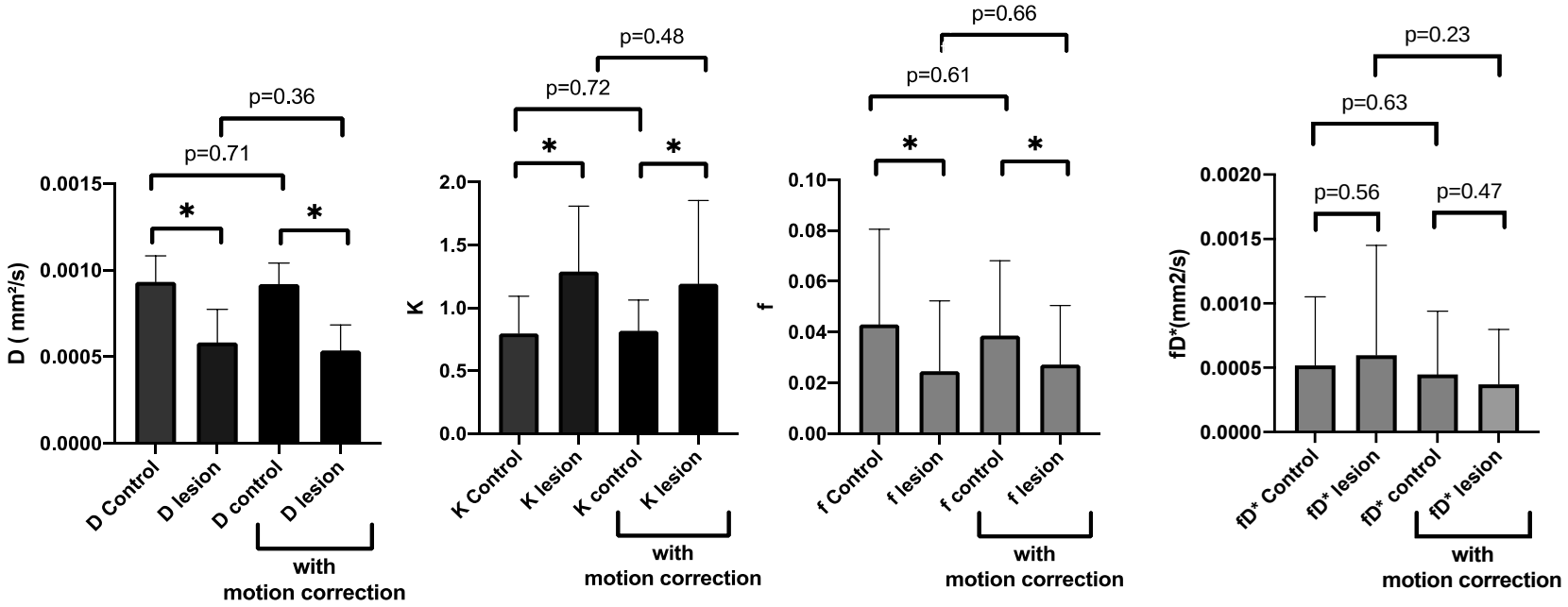

(b)

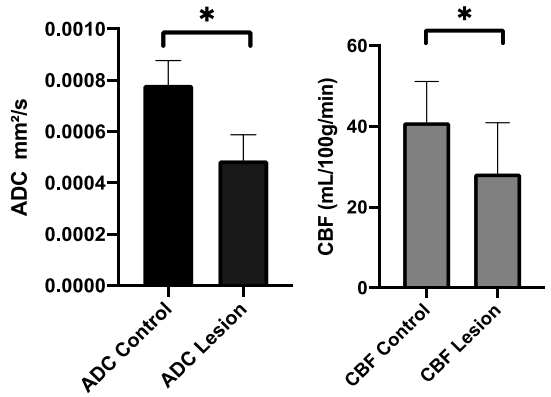

(a) C
o
m
p
a

rison of DKI-IVIM parameters between ischemic areas and contralateral healthy tissues before and after motion correction.
(b) Comparison of ADC and CBF parameters between ischemic areas and contralateral healthy tissues.

Figure 5

Scatter plots and Pearson correlation coefficients between ADC and IVIM diffusion parameters D and K: ADC versus D (a), ADC versus K (b) and between K and D (c). Data points are mean values from the whole lesion and contralateral ROIs across all the patients.

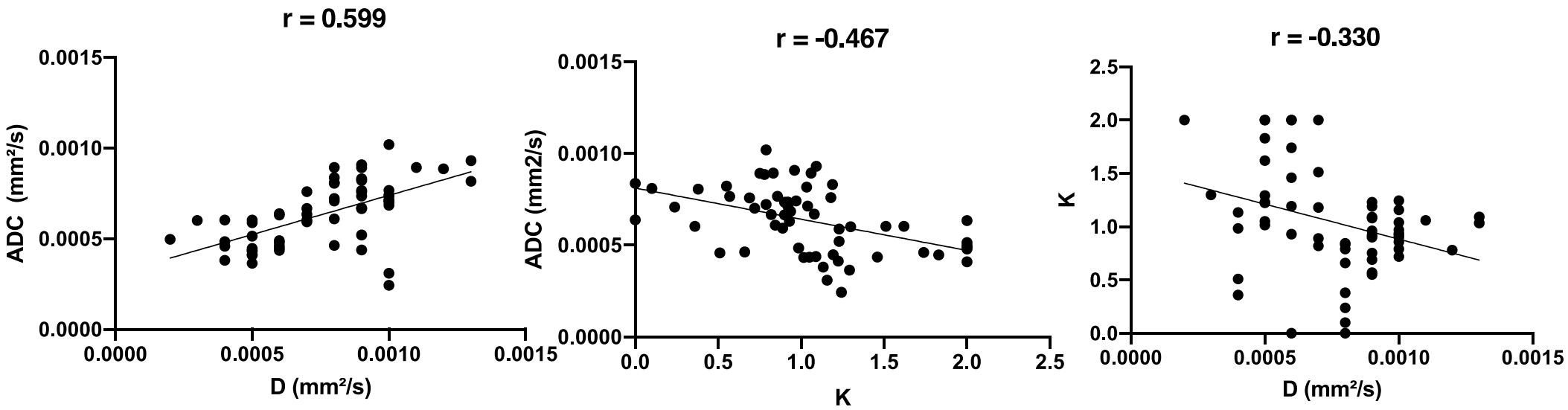

Author Statement

Aude Pavilla : Investigation, Methodology, Software, Formal analysis, Data Curation, Writing- Reviewing and Editing

Giulio Gambarota : Conceptualization, Methodology

Aissatou Signaté : Investigation, Validation

Alessandro Arrigo : Conceptualization, Methodology

Hervé Saint-Jalmes : Conceptualization, Methodology, Software, Formal analysis, Validation, Reviewing.

Mehdi Mejdoubi : Conceptualization, Methodology, Validation, Reviewing

Highlights

- DKI-IVIM imaging at 3T enables simultaneous measurement of K, D, f and fD*in acute/subacute stroke.
- ADC was significantly positively correlated with D and significantly negatively correlated with K in the ischemic lesions. A significant negative correlation was also found between D and K.
- Combined f/fD*/D/K offers noninvasively a potential enhanced ischemic lesions characterization in a shorter acquisition time than DWI and ASL do separately.